RESEARCH ARTICLE

Overlooked species diversity in the hyper-arid Sahara Desert unveiled by dryland-adapted lizards

André Vicente Liz[1,2,3,4] | Dennis Rödder[4] | Duarte Vasconcelos Gonçalves[1,3,5] | Guillermo Velo-Antón[1,3,6] | Pedro Tarroso[1,3,7] | Philippe Geniez[8] | Pierre-André Crochet[9] | Silvia B. Carvalho[1,3] | José Carlos Brito[1,2,3]

[1]CIBIO, Centro de Investigação em Biodiversidade e Recursos Genéticos, InBIO Laboratório Associado, Universidade do Porto, Vairão, Portugal

[2]Faculdade de Ciências, Departamento de Biologia, Universidade do Porto, Porto, Portugal

[3]BIOPOLIS Program in Genomics, Biodiversity and Land Planning, CIBIO, Vairão, Portugal

[4]LIB, Museum Koenig, Bonn, Leibniz Institute for the Analysis of Biodiversitiy Change, Bonn, Germany

[5]CIIMAR, Centro Interdisciplinar de Investigação Marinha e Ambiental, Terminal de Cruzeiros de Leixões, Matosinhos, Portugal

[6]Departamento de Ecoloxía e Bioloxía Animal, Grupo GEA, Universidade de Vigo, Vigo, Spain

[7]Institute of Evolutionary Biology, CSIC-Universitat Pompeu Fabra, Barcelona, Spain

[8]CEFE, Univ Montpellier, CNRS, EPHE-PSL University, IRD, Biogéographie et Ecologie des Vertébrés, Montpellier, France

[9]CEFE, CNRS, University of Montpellier, EPHE, IRD, Montpellier, France

Correspondence
André Vicente Liz, CIBIO/InBIO, Centro de Investigação em Biodiversidade e Recursos Genéticos da Universidade do Porto, Instituto de Ciências Agrárias de Vairão, Rua Padre Armando Quintas 7, 4485-661 Vairão, Portugal.
Email: andre.vicente.liz@cibio.up.pt

Abstract

Aim: Hyper-arid sandy and rocky fields rank among the least biologically diverse habitats of the desert biome, yet knowledge of local biodiversity patterns is also extremely poor. In the Sahara Desert, palaeoclimate oscillations affected the extent of hyper-arid habitats, but it is unclear how these dynamics determined the evolution and distribution of local specialists. Herein, we assessed cryptic diversity, diversification patterns and spatial connectivity within a Sahara-widespread group of dryland-adapted lizards.

Location: Sahara-Sahel ecoregions.

Taxon: *Acanthodactylus scutellatus* species group.

Methods: Inter- and intraspecific phylogenetic structure, divergence times, spatial genetic patterns and cryptic diversity were assessed using nuclear and mitochondrial loci. The effects of topography and land cover on phylogeographic structure and diversity were tested with generalized linear models. Interspecific hybridization was evaluated using 11 microsatellites across the group's major sympatry zone, predicted based on ecological niche models.

Results: Species of *Acanthodactylus scutellatus* group exhibit Late Miocene origins, followed by extensive intraspecific divergence throughout the Pliocene. The northern Sahara worked as a major diversification hotspot, harbouring a patchwork of small-ranged, divergent lineages. These lineages are parapatric or sympatric and present concordant nuclear and mitochondrial differentiation, suggesting species status. Genetic connectivity increases in southern latitudes, with wide-ranging lineages spanning from the Red Sea to the Atlantic coast. Within these potential corridors, mountain outskirts and sand fields in the Sahara interior seemingly acted as origins for recent population expansions. Genetic diversity and connectivity are favoured by terrain roughness and soft-sand cover respectively. Three species inhabit the Atlantic Sahara sympatry zone without evidence of gene flow.

Main conclusions: Overlooked species-level diversity within a major specialist group of Sahara drylands exposes the recurrent knowledge shortfalls present in hyper-arid

desert environments. Humidity and sandy habitat shifts triggered potential successions of population isolation and re-connectivity, which favoured cladogenesis in northern desert regions and population expansions across southern east–west corridors.

KEYWORDS
climatic cycles, gene flow, hidden diversity, lizard, North Africa, phylogeography, sand corridor, speciation, sympatry, xeric

1 | INTRODUCTION

Deserts and arid zones present the lowest species richness among the Earth's biomes (Hughes et al., 2021). Biased by this poor diversity, we tend to perceive desert biomes as vast and homogeneous environments devoid of life, which consequently attract less research and conservation interest (Durant et al., 2012) despite providing key global ecosystems services (e.g., climate regulation [Barkley et al., 2022]). However, many deserts experienced a dynamic geological past (Pepper & Keogh, 2021) that generated high levels of endemism (Šmíd et al., 2021) and unique biodiversity adaptations to aridity (Ward, 2016). The Sahara Desert, together with the neighbouring Sahel (Figure 1), is the largest warm desert on Earth, exhibiting a wide variety of climate and topography (Brito et al., 2014). It spans poor and low developed areas where remoteness, armed conflicts and socio-political instability have undermined surveying and research for decades (Brito et al., 2018). Because of this, Saharan biodiversity is possibly the least known among world deserts (Brito & Pleguezuelos, 2020). Yet, severe anthropogenic (Durant et al., 2014) and climatic (Soultan et al., 2019) disturbances heighten the urgency to properly catalogue its extant species, understand their biogeographic and evolutionary history and identify priority conservation zones (Brito et al., 2016).

The inventory of Saharan species diversity has long relied on external morphology (e.g., Crochet et al., 2003), which can be misleading given that species' morphology tends to converge due to the harsh desert environments. This has led to a low-resolution taxonomy where distant populations without obvious morphological differences were aggregated under the same unit (e.g., *Mesalina* spp. [Pizzigalli et al., 2021]), thus creating an impression of low biological turnover across the desert. The implementation of molecular tools (reviewed by Brito et al., 2014 but see Velo-Antón et al., 2022) led to the identification of unrecognized diversity within several wide-ranging species (e.g., *Tropiocolotes tripolitanus* [Machado et al., 2020]), questioning the presumed homogeneity of the Sahara. However, research efforts are largely biased towards the milder and more accessible areas (mountains [e.g., Liz et al., 2021] and desert margins [e.g., Velo-Antón et al., 2018]; Weiss et al., 2018), while the most xeric habitats (i.e., Aridity Index <0.03 [Ward, 2016]; Figure 1) remain genuinely understudied and perceived as biologically uniform (Brito et al., 2014). These habitats exhibit more geological and ecological diversity than what is often realized (Brito & Pleguezuelos, 2020),

harbouring specialists of a single type of substratum such as sand dunes (*ergs*; e.g., *Scincus* spp. [Šmíd et al., 2020]) or rocky plains (*regs* or *hammadas*; e.g., *Uromastyx* spp. [Tamar et al., 2017]). Incomplete knowledge negatively impacts conservation efforts due to biased biodiversity metrics (Brito et al., 2016); thus, phylogeographic studies of wide-ranging xeric species are needed to assess the extent of knowledge shortfalls in the hyper-arid Sahara.

Speciation events and current biodiversity distribution patterns in the Sahara have been influenced by dry/humid cycles since the Late Miocene (Drake et al., 2011). The land cover changes that resulted from climatic oscillations likely elicited contrasting responses from taxa with different ecological requirements (Brito et al., 2014). Mountains are traditionally depicted as refugia and speciation centres for mesic species (e.g., *Agama* spp. [Gonçalves, Pereira, et al., 2018]), but it is unclear how this pattern applies to dryland specialists. These species may have experienced isolation and divergence in xeric lowlands, which were fragmented during green Sahara periods (such as the African Humid Period ~6 kya). However, the climatic cores of xeric habitats could have become too extreme to allow long-term population persistence during arid phases, which would imply that xeric refugia are instead located on the edge of these habitats or on the outskirts of mountain regions. The intermittent expansion and interconnection of sand fields opened opportunities for the dispersal of *erg* specialists, leading to rapid trans-Saharan radiations (e.g. *Scincus* spp. [Šmíd et al., 2020]). No comprehensive assessment exists on the location of these corridors, although the current distribution of some sand-adapted lineages (e.g., *Stenodactylus petrii* [Metallinou et al., 2012]) suggests that they stretched from east to west of the continent throughout southern desert regions, potentially linked to southward desert expansions during arid Sahara phases (e.g., Last Glacial Maximum ~21 kya; Steele, 2007). This contrasts with a widespread pattern of range breaks across northern regions (e.g., *Chalcides* spp. [Carranza et al., 2008]), where humid barriers between xeric habitats (Scerri et al., 2014) likely prompted population fragmentation.

Wide-ranging dryland-adapted taxa with high ecological or morphological variation are ideal to investigate the major drivers of diversification in xeric species. *Acanthodactylus* fringe-toed lizards present such high diversity, holding similar potential for eco-evolutionary studies to *Podarcis* spp. in Europe (Yang et al., 2021), but are still poorly studied. The *A. scutellatus* species group (Boulenger, 1921; hereafter, Scutellatus group) comprises
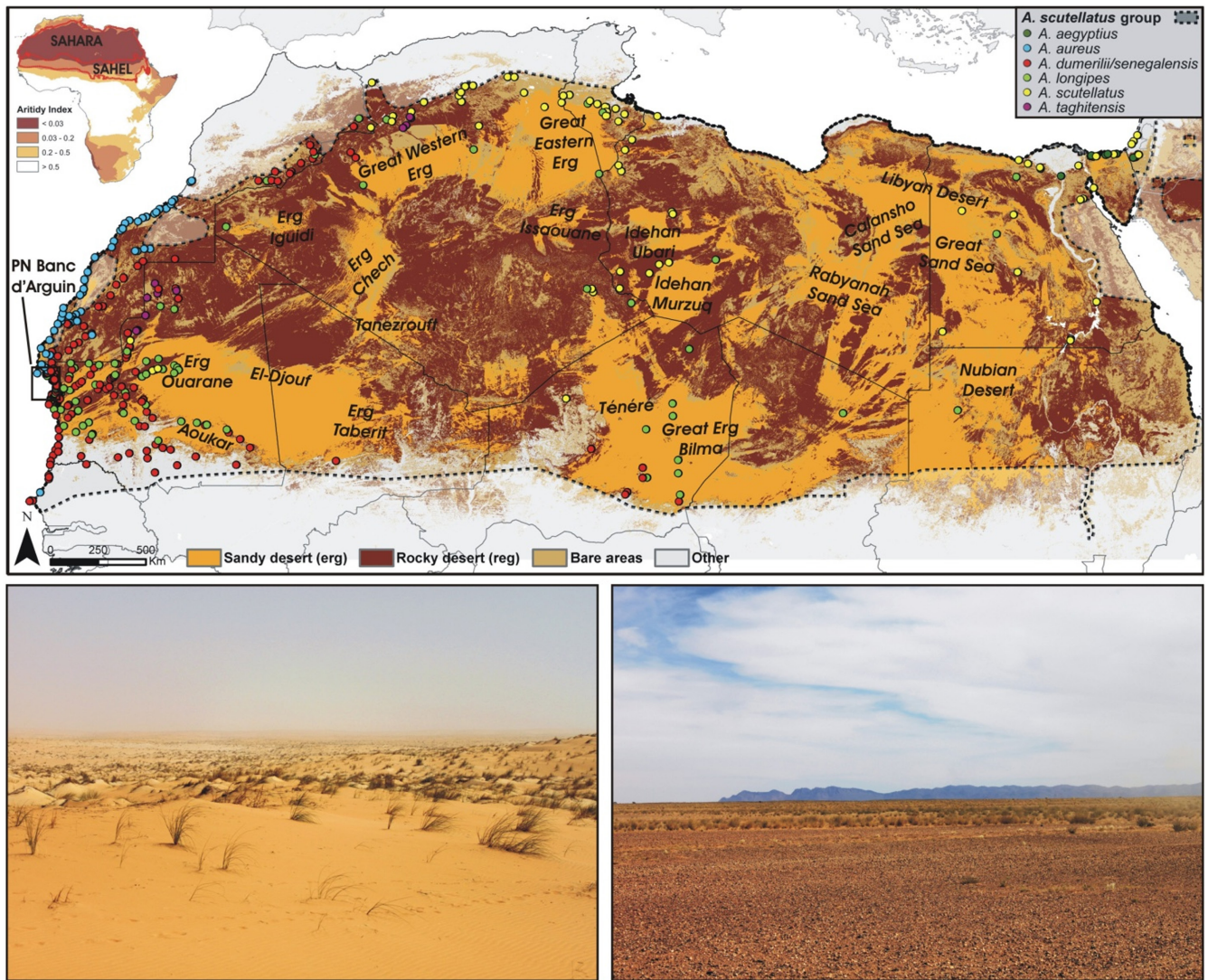
FIGURE 1 Top: Land cover map of the study area including the three desert-type variables (Bicheron et al., 2009), with main *ergs* indicated in bold. Circles represent samples of *Acanthodactylus scutellatus* group used in the phylogenetic analysis, with species differentiated by colour. The dashed polygon represents the group's range (modified from Roll et al., 2017). The sympatry zone Parc National du Banc d'Arguin targeted in the population genetic analysis is highlighted. Map projection: WGS84. Bottom: Photographs of two hyper-arid habitats, the *erg* Aoukar (left) and the *reg* Gleib el Outat (right) in Mauritania.

seven recognized species (*A. aegyptius*, *A. aureus*, *A. dumeri-lii*, *A. longipes*, *A. scutellatus*, *A. senegalensis* and *A. taghitensis*) which are abundant and conspicuous across xeric environments of North Africa and the Middle East (Figure 1; Figure S1.1 in Appendix S1; Sindaco & Jeremčenko, 2008), and easily sampled in accessible regions of the hyper-arid Sahara. Most species are linked to sandy habitats, but their ecology varies from the soft-sand specialist *A. longipes* to the more generalist *A. scutellatus*. The only exception is *A. taghitensis*, which only occurs in gravel plains. Despite the group's potential as a study system, base-line knowledge of the species' distributions and phylogenetic relationships is still preliminary (Harris & Arnold, 2000; Psonis et al., 2016; Tamar et al., 2016) or limited to small areas (Velo-Antón et al., 2018). These species show both a high interspecific morphological conservatism and a large amount of intraspecific

variation (Arnold, 1983; Salvador, 1982), which hampers morphological identification and systematics. The occurrence of morphologically intermediate specimens has raised suspicion of interspecific hybridization (Crochet et al., 2003) despite their million-year-old divergence (Tamar et al., 2016). As with many other groups of small vertebrates, distinguishing evolutionary sensible units from geographical variations in morphology requires molecular tools.

The main objective of this study is to understand the biogeographic and ecological drivers of evolutionary diversity in the Scutellatus group across the Sahara-Sahel. To do so, we combine ecological niche modelling with phylogenetic and population genetic analyses. First, we examine the distribution of genetic diversity at inter- and intraspecific levels, unveiling a considerable amount of previously unrecognized diversity, to: (1) identify

areas of higher diversity and distinctiveness (i.e., diversification hotspots); and (2) map shared genetic diversity (i.e., recent connectivity). Given palaeogeomodels and allopatric lineage distributions in other sand-dwelling taxa across northern Sahara, we expect multiple diversification hotspots in this region resulting from recurrent fragmentation of xeric habitats. In contrast, we expect widespread connectivity in the south of the Sahara and in the Sahel, where fewer humid barriers among xeric habitats exist as a result of great sand expansion dynamics during the Plio-Pleistocene. Secondly, we (3) investigate the role of speciation in generating evolutionary diversity in the Scutellatus group, by examining if recent admixture takes place in an area of sympatry where the number of overlapping evolutionary units is especially large.

2 | MATERIALS AND METHODS

2.1 | Study region and data collection

Our study area comprises xeric areas of North Africa and adjacent portions of the Middle East (Figure 1). It includes the ecoregions Sahara Desert and parts of the Sahel savannah, as well as neighbouring Mediterranean steppes and dry woodlands in North Africa and the xeric shrublands from Sinai and southern Levant in the Middle East (Dinerstein et al., 2017). For population genetics analyses, we selected an area in coastal Mauritania, the Parc National du Banc d'Arguin (PNBA; Figure 1), where *A. aureus*, *A. dumerilii*, *A. longipes* and *A. senegalensis* are sympatric (Roll et al., 2017; and see Section 3.3) and morphologically intermediate individuals have been reported (Crochet et al., 2003).

For phylogenetic analyses, we used 542 georeferenced tissue samples collected during field expeditions between 2003 and 2019 or acquired from museum collections, representing all the currently accepted species within the Scutellatus group (Figure 1; Table S2.1 in Appendix S2). Previously published sequences from additional 124 georeferenced samples were retrieved from GenBank (Tamar et al., 2014; Tamar et al., 2016; Velo-Antón et al., 2018). For ecological modelling, we gathered species' occurrence records from fieldwork, museums and bibliography, totalling 930 observations (Table S2.1). Models targeted all recognized species except for the monophyletic unit made of *A. dumerilii* and *A. senegalensis* (*A. dumerili/senegalensis* hereafter), following the results of the genetic analyses (see Section 3.1). Observations lacking genetic diagnosis (28%) were only kept if they were located in congruent localities and the taxonomic identification was not dubious. For population genetics, we used a subset of 208 samples from the sympatry zone (Table S2.1). These samples were preliminarily identified based on external morphological characters (scalation and colour pattern; Crochet et al., 2003) and included typical morphotypes for the putative species *A. aureus*, *A. longipes*, *A. dumerilii* and *A. senegalensis*, as well as morphologically intermediate individuals between the latter two taxa.

2.2 | Ecological variables

For ecological models, we used multitemporal remote sensing variables derived from preprocessed data of two NASA satellites (dataset MODIS v4; EDENext project). These sources covered the following bands and derived products: middle infra-red (MIR [Jensen, 2007]); day and night time land surface temperatures; normalized difference vegetation index (NDVI [Tucker, 1979]); and enhanced vegetation index (EVI [Huete et al., 1997]). Additionally, we included the eight precipitation-related bioclimatic variables (bio12–bio19); WorldClim 2.0; Fick & Hijmans, 2017) and three desert-specific land cover types (Globcover dataset; Bicheron et al., 2009): *erg*, *reg* and bare-area. All variables were downloaded or upscaled to 30 arc-sec resolution (∼1 × 1 km) and cropped to the study area. Pairwise correlations were assessed based on Spearman's $R^2 < 0.7$, selecting a final subset of 18 low-correlated variables (Table S2.2). Extended details in variable selection and processing are given in Text S3.1 in Appendix S3.

2.3 | DNA extraction, amplification, sequencing and genotyping

Standard protocols for DNA extraction, amplification and sequencing were followed (see details in Text S3.2). For phylogenetic analyses, two mitochondrial fragments, the 12S ribosomal RNA (12S; 368 base pairs) and the cytochrome-b (Cytb; 377 bp), and the nuclear fragment oocyte maturation factor MOS (C-mos; 468 bp) were targeted. Primers and PCR conditions are given in Tables S2.3 and S2.4 respectively. For population genetic analyses, a selection of 14 microsatellites previously developed for the Scutellatus group (Lopes et al., 2015; Table S2.5) was used to genotype the samples from the sympatry zone.

2.4 | Phylogenetic inference, divergence dating and lineage delimitation

Sequences were arranged into concatenated mitochondrial (mtDNA; *n* = 555; 745 bp) and cytonuclear (mt-nuDNA; *n* = 482; 1213 bp) datasets (Table S2.1), including samples successfully sequenced for all target markers. Outgroups included representatives of the other two major *Acanthodactylus* clades (Tamar et al., 2016), as well as of the closely related *Mesalina* genus (Table S2.6).

Bayesian Inference (BI) and Maximum Likelihood (ML) analyses were performed with the mt-nuDNA dataset, using BEAST v.1.10.4 (Suchard et al., 2018) and RAXMLGUI (Silvestro & Michalak, 2012) respectively. BEAST was run on the CIPRES gateway (Miller et al., 2010) in two independent runs of 10^8 generations, sampling at every 10^4, with unlinked substitution and clock models (Drummond et al., 2006), a constant population size coalescent tree prior (Kingman, 1982) and considering ambiguities in the nuclear partition. For ML analyses,

1000 bootstrap replications were performed. Extended details on the phylogenetic analyses are given in Text S3.3 and Table S2.7. Nodes in the resultant BI and ML trees were considered well supported at posterior probabilities >0.95 and bootstrap values >85 respectively.

The BI phylogenetic inference was time calibrated following the strategy of Tamar et al. (2016). Another mt-nuDNA alignment was produced using representatives of all intraspecific lineages ($n = 74$; Table S2.1) and adding sequences of *Gallotia*, *Psammodromus* and *Podarcis* spp. (Table S2.6). Biogeographic calibration events were the end of the Messinian Salinity Crisis and the ages of the Canary Islands (Table S2.8). Node split times were estimated in BEAST v.1.10.4 (Suchard et al., 2018; see Table S2.7 for detailed settings).

Previously published lineages of *A. aureus* (Velo-Antón et al., 2018) were the baseline threshold to delimit intraspecific lineages within the Scutellatus group. Lineages were defined as those reciprocally monophyletic, well-supported clades in the BI mt-nuDNA tree, with splits from sister taxa older than the most recent lineage split within *A. aureus* (1.84 Mya). Our study includes a similar set of genetic markers (excluding cytochrome oxidase I) to those used in the original delimitation (Velo-Antón et al., 2018). Despite its limitations, this strategy works well for assessing intraspecific diversity patterns across the study area, and the general patterns recovered remain consistent when applying more conservative thresholds (e.g. first split within *A. aureus* 3.09 Mya).

Intraspecific haplotype networks were constructed for C-mos and the mtDNA marker sequenced for the most samples (12S; $n = 635$; Table S2.1) using TCS v.1.21 (Clement et al., 2002), with 95% parsimony threshold and visualized using TCSBU (Santos et al., 2015). The nuclear haplotypes were reconstructed for each species using the PHASE implementation in DNASP 5.10.01 (Librado & Rozas, 2009), with 10^4 iterations and 10^3 of burn-in. Pairwise genetic distances (p-distances) between species and lineages were calculated on 12S using MEGA v.7 (Tamura et al., 2013), based on Kimura-2 parameter model.

2.5 | Spatial interpolations of genetic data

Intraspecific nucleotide diversity was calculated using the mtDNA dataset with 'Pegas' R package (Paradis, 2010). For each species, we measured the pairwise distance between samples and identified the maximum nearest-neighbour distance. This distance was set as a radius of a neighbourhood from which a set of samples was selected to calculate average nucleotide diversity (thus guaranteeing that at least two samples were included in each neighbourhood). To reduce bias due to the different number of samples within the neighbourhood of each location, from the set of haplotypes within the neighbourhood, two of them were iteratively resampled with replacement (1000 replicates) to calculate pairwise nucleotide diversity. Values were averaged across replicates to obtain an estimation of genetic distinctiveness for each mtDNA haplotype in relation to the whole species' diversity. To predict patterns across species' ranges, genetic distinctiveness was spatially interpolated with the idw function of 'phylin' R package (Tarroso et al., 2019), using two spatial grid sizes to account for differences in species' range sizes and sampling: 10x10 km for *A. aegyptius*, *A. aureus*, *A. dumerilii/senegalensis* and *A. taghitensis*; and 50x50 km for *A. longipes* and *A. scutellatus*. Projections were clipped to species' ranges (Roll et al., 2017).

2.6 | Landscape drivers of genetic structure and diversity

Generalized linear models (GLMs; Matthiopoulos, 2011) with normal errors were fitted in R to test the effect of different topographic and land cover variables on genetic diversity and connectivity. Two independent approaches were followed, where the response variables were mtDNA haplotype distinctiveness ('diversification model') and diameter of lineage Minimum Convex Polygon (MCP; 'connectivity model') respectively. As predictors for the diversification model, absolute values of altitude and index of terrain roughness (Title & Bemmels, 2018), as well as coverage percentage of *erg*, *reg* and bare-area (Bicheron et al., 2009), were extracted from each haplotype locality, excluding duplicates; for the connectivity model, averages of the same five variables were calculated within MCPs of all lineages using the Zonal Statistics tool of ArcGIS v.10.5 (ESRI, 2006). Additionally, species was included as a predictor in both models, while nearest-neighbour distance and number of lineage samples were also included in the diversification and connectivity models respectively. Model comparisons were performed using different combinations of topographic and land cover predictors based on the Akaike information criterion (AIC; Akaike, 1998), in order to build the best-fitting models including only one topographic and one land cover predictor. Lineages with a sample count <3 were excluded from the connectivity model because it is not possible to construct an MCP for these lineages.

2.7 | Ecological niche modelling

For each species, the initial pool of records was tested for spatial clustering to account for potential sampling bias and to avoid model overfitting (Boria et al., 2014) using the ecospat.mantel.correlogram function of 'ecospat' R package (Di Cola et al., 2017), and thinned accordingly with 'spThin' (Aiello-Lammens et al., 2015). The final sets contained: 37 records of *A. aegyptius* (minimum distance between records: 7 km); 47 of *A. aureus* (16 km); 82 of *A. dumerilii/senegalensis* (52 km); 77 of *A. longipes* (67 km); 70 of *A. scutellatus* (49 km); and 17 of *A. taghitensis* (18 km).

The contemporary ecological niche of each species was modelled using BIOMOD2 (Thuiller et al., 2021). Detailed procedures are given in Text S3.4. Six algorithms were chosen to reduce the uncertainties associated with modelling techniques (Thuiller et al., 2019). Ten model replicates were run for each of the six algorithms for each species, using 80% of presence data for training.

A final ensemble model was built using model replicates for which the area under the receiver operating characteristic curve (AUC; Fielding & Bell, 1997) was >0.7. Replicates were weighted proportionally according to predictive performance (Marmion et al., 2009).

Ensemble models were clipped to species' ranges (Roll et al., 2017). Projections of ensemble models were assessed using clamping masks to identify and minimize errors in spatial extrapolations beyond the training range of the models (Elith et al., 2010). Ensemble models were converted to binary (i.e., suitable/unsuitable habitat) using the TSS cut-off threshold. Binary projections between species were overlapped in ArcGIS 10.5 (ESRI, 2006) to infer sympatry zones.

2.8 | Microsatellite analyses

Evidence of stuttering, null alleles and allelic dropouts was assessed using MICRO-CHECKER 2.2.3 (Van Oosterhout et al., 2004). Tests for genotypic linkage disequilibrium (LD) and Hardy–Weinberg equilibrium (HWE) were assessed in GENEPOP'007 (Rousset, 2008), with individuals grouped based on the three recovered phylogenetic clades (see Section 3.1). Subsequent sequential Bonferroni corrections were applied in both cases.

Bayesian population clustering analyses were conducted in STRUCTURE 2.3.4 (Pritchard et al., 2000) to estimate the optimal number of clusters, assign individuals to each resultant cluster and infer the differentiation and relationships among clusters (see details in Text S3.5). All genotyped samples were also sequenced for at least one phylogenetic marker except for four cases of failed amplification in A. aureus. Potential admixture was examined by assessing concordance between mtDNA and microsatellites species assignment and by examining individual ancestry based on microsatellites clustering. Admixed individuals would indicate contemporary hybridization while cytonuclear discordance in species assignment would suggest past introgression.

3 | RESULTS

3.1 | Phylogenetic inferences

The phylogenetic mt-nuDNA trees revealed five major, well-supported, monophyletic clades, partially matching with six species of the Scutellatus group (Figure 2; Figures S1.2 and S1.3). *Acanthodactylus aureus*, *A. taghitensis*, *A. longipes* and *A. scutellatus* were recovered as reciprocally monophyletic clades that were largely consistent with the preliminary field identification of the specimens. Samples identified as *A. dumerilii* and *A. senegalensis* were placed together in a single clade. Samples of *A. aegyptius* formed a monophyletic group within *A. longipes*. The relationships between the major clades were strongly supported except for the position of *A. taghitensis*. Divergence estimates indicate that the diversification

of the group started in the Middle Miocene (Figures 2; Figure S1.4) with the basal branching of *A. aureus* ~16.9 Mya (95% HPD: 12.7–21.3). All remaining major clades split throughout the Late Miocene. Within major clades, diversification onsets were placed in the Late Miocene (around 7.6–7.9 Mya) for *A. longipes* and *A. scutellatus*, and in the Early Pliocene (4.3–5.1 Mya) for *A. taghitensis* and *A. dumerilii/ senegalensis*. Diversification of *A. aureus* started in the Late Pliocene. All major clades presented distinguishable nuclear haplogroups except for *A. dumerilii/senegalensis*, in which some alleles from the intraspecific lineage 'NW Sahara' were embedded within *A. scutellatus* (Figure S1.5).

The five major clades include several lineages with variable range sizes (Figure 2) and degree of genetic differentiation (Figures S1.6 and S1.7a–S1.7c; Table S2.9). The *A. aureus* clade includes three parapatric lineages distributed along the Atlantic Sahara but lacking evidence for nuclear differentiation (concordant with Velo-Antón et al., 2018). Samples of *A. taghitensis* are divided into two allopatric lineages, one from each of the disjoint occurrence areas in Algeria and Mauritania, exhibiting high mtDNA distance and lack of nuclear allele sharing. The *A. longipes* samples form a diverse pan-Saharan complex composed of eight lineages, including *A. aegyptius*, with strongly supported relationships except for the position of lineage 'Grand Western Erg'. Two of these lineages range from the Central Sahara-Sahel to the Red Sea ('E Sahara-Sahel') and Atlantic ('W Sahara-Sahel South') coasts, respectively; two others span over a wide latitudinal axis ('Central Sahara' and 'W Sahara-Sahel Inland'); and all the remaining ones are found in smaller areas across northern Sahara. The three basal lineages of the complex ('Tunisia', 'Grand Western Erg', 'A. aegyptius') exhibit parapatric distributions relative to adjacent lineages and present remarkable mtDNA distances and private nuclear alleles that are not shared between them or with any other lineage. The *A. scutellatus* clade is another pan-Saharan complex structured in 10 lineages, with mostly unresolved relationships. Among this diversity, one lineage is broadly distributed from Mauritania to Egypt ('Pansaharan'), another from the Central Sahara to the Red Sea ('N Sahara') and the rest show restricted distributions across northern Sahara and the Central Sahara highlands, where they occur mostly in parapatry or even in sympatry. All lineages are separated by several mtDNA mutation steps, whereas four lineages also present private nuclear alleles and two only share one allele. The *A. dumerilii/senegalensis* clade includes four lineages in two main branches, with all relationships resolved except for the split between lineages 'Merzouga' and 'NW Sahara'. One branch is formed by a widespread lineage, spanning over the western Sahara-Sahel throughout the southern distribution of *A. dumerilii* and the entire range of *A. senegalensis*. The other branch is highly diverse, harbouring three seemingly sympatric lineages restricted to a small area on the Moroccan–Algerian border. These lineages exhibit high nuclear differentiation in relation to the other main branch of *A. dumerilii/ senegalensis*. Lineage 'Merzouga' is represented by a unique nuclear haplotype that is very distant from those of the other two local lineages. Within lineage 'NW Sahara', one nuclear allele is highly separated from the others, being placed close to lineage 'Merzouga'.
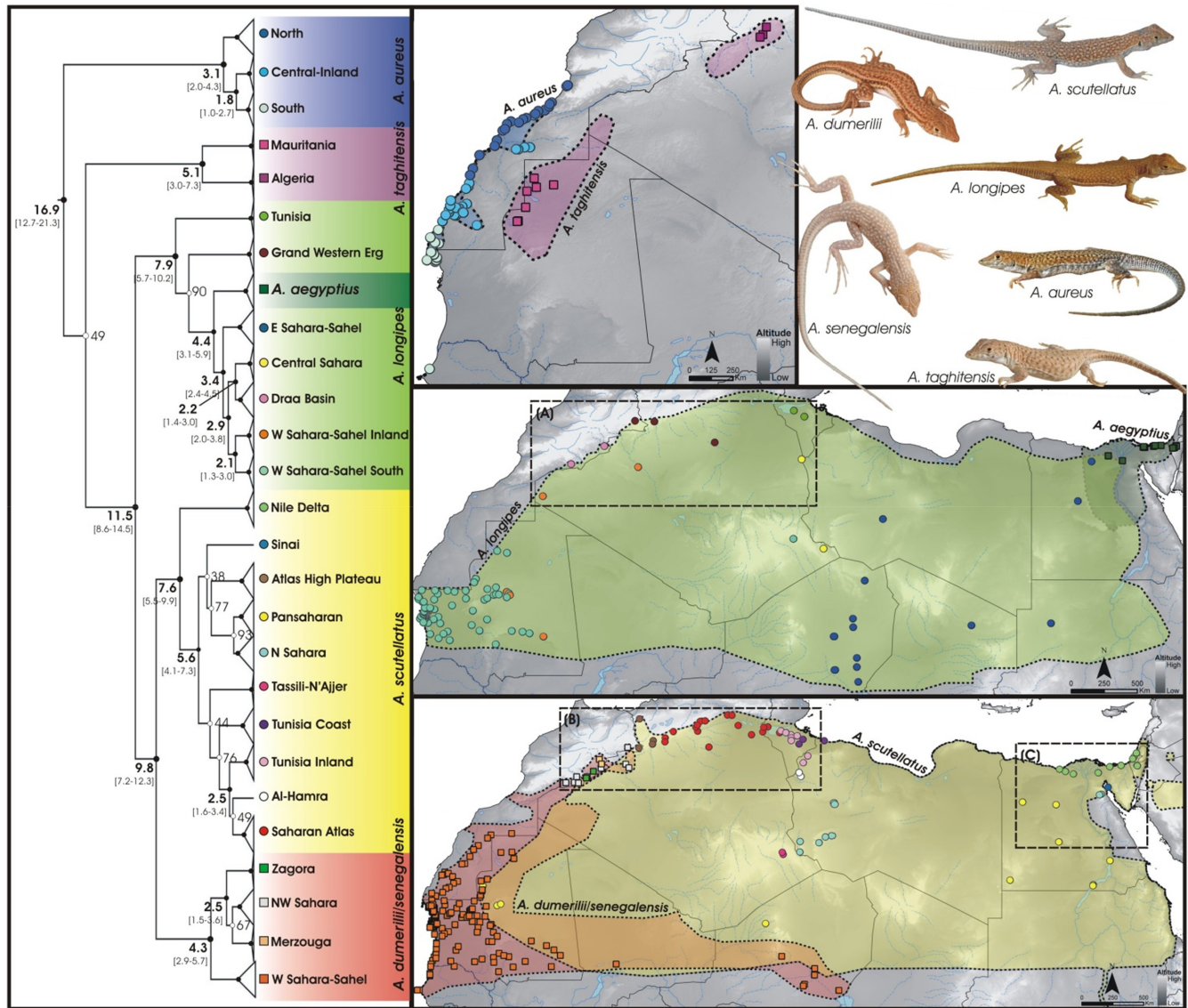
FIGURE 2 Left: Time-calibrated Bayesian mt-nuDNA tree showing species and intraspecific lineages within *Acanthodactylus scutellatus* group, obtained from the concatenation of two mtDNA fragments and one nuclear gene (12S, Cytb, and C-Mos; 1213 bp). Black dots represent supported nodes, with posterior probabilities (pp) >0.95; white dots represent unsupported nodes, where pp values are indicated at the right. Split times (Mya) are given in bold for supported nodes (95% HPD between brackets). See Figure S1.2 for full sample names. Right: Distribution maps of intraspecific lineages. Dashed rectangles depict small-ranged lineage hotspots zoomed in Figure S1.7. Map projections: WGS84.

3.2 | Patterns and drivers of genetic structure and diversity

Lineage range size increases at lower latitudes, contrasting with higher fragmentation in northern regions (Figure 3; Figures S1.7d–S1.7f). High levels of mtDNA haplotype distinctiveness were found in the north-western Saharan edge for *A. longipes*, *A. scutellatus* and *A. dumerilii/senegalensis* (Figure 3), specifically in areas between the High and Saharan Atlas, the Great Algerian *ergs* and the chott palae-olakes. Distinctiveness also increased around Ténéré *erg* (Niger), the Western and Sinai Deserts (Egypt), the Fezzan Mountains and palae-olakes (Libya) and the Tassili-N'Ajjer (Algeria) for *A. scutellatus;* in the Adrar (Mauritania) and Bilma *erg* (Niger) for *A. longipes;* and around Aouker *erg* and palaeolakes (Mauritania) for *A. dumerilii/senegalensis*.

The GLMs including *erg* substrate and terrain roughness as predictors presented the lowest AIC to explain variations in lineage range size and haplotype distinctiveness (Table S2.10). Among these predictors, *erg* substrate and terrain roughness positively influence lineage range size and haplotype distinctiveness respectively (Figure 3; Table 1).

3.3 | Ecological niche suitability

Ecological niche models achieved good performance (AUC ranged between 0.80 and 0.97; Table S2.11). Species' potential distributions overall matched with their known ranges (Figures S1.8–S1.10). However, *A. longipes* and *A. scutellatus* presented some discrepancies,
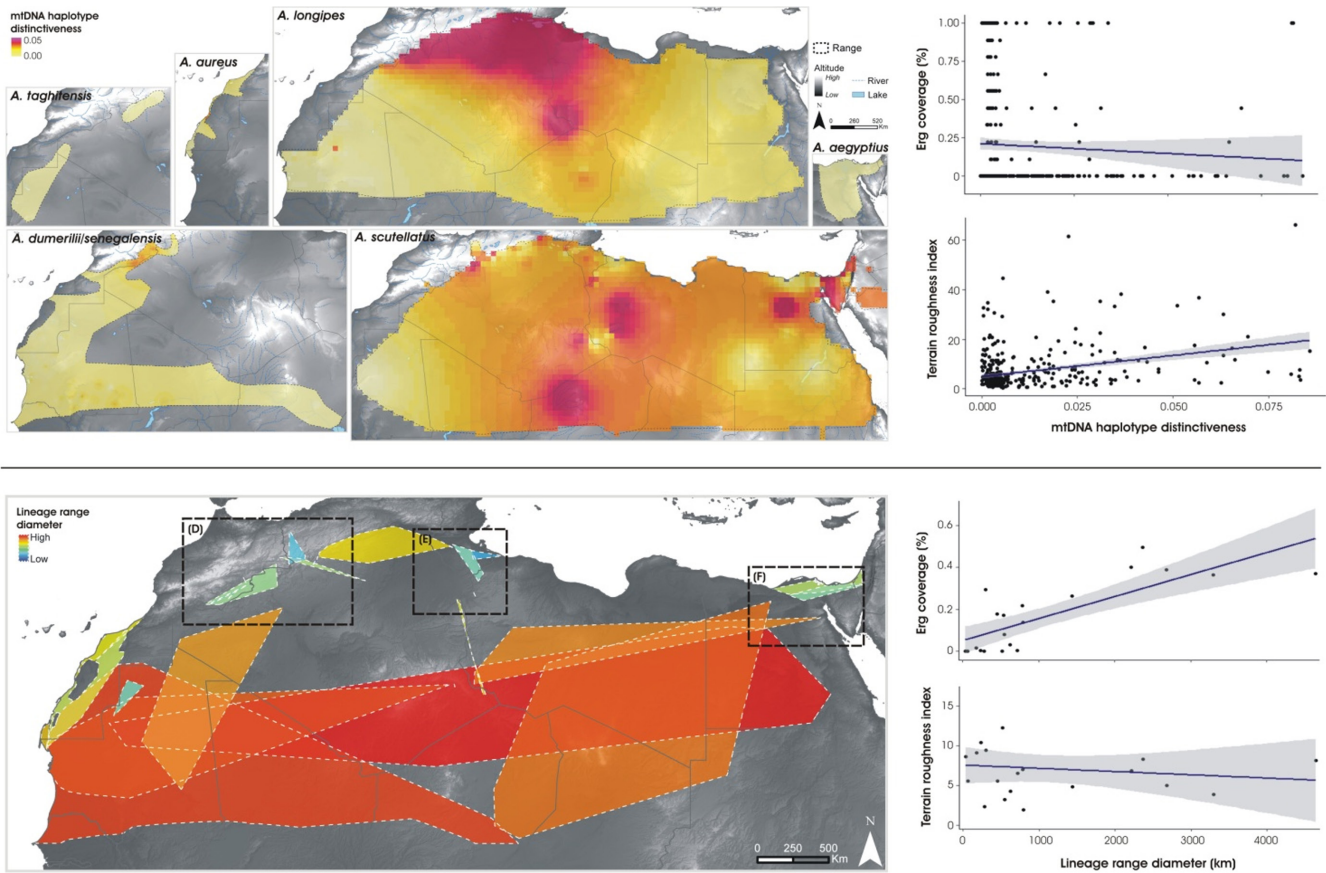
FIGURE 3 Top: Interpolations of mtDNA haplotype distinctiveness for species of *Acanthodactylus scutellatus* group, based on nucleotide diversity of two concatenated markers (12S and Cytb; 745 bp). The linear relationships of haplotype distinctiveness with terrain roughness and soft-sand coverage, at each sampling point, are shown at the right. Bottom: Minimum convex polygons (MCPs) of intraspecific lineages. Dashed rectangles depict small-ranged lineage hotspots zoomed in Figure S1.7. The linear relationships of MCPs' diameter with MCP's average terrain roughness and soft-sand coverage are shown at the right. Grey bands in the regression plots indicate confident intervals (CI: 95%). Map projections: WGS84.

as revealed by the denser concentration of suitable habitats in southern and northern areas of the Sahara respectively. Environmental predictors with the greatest contribution to models varied between species (Table S2.12), but some of those derived from day and night time land surface temperature consistently presented high contribution.

The main sympatry zone was predicted in the western Sahara-Sahel (Figure 4), covering the Atlantic Sahara ecoregion and the Adrar plateau, where up to four species may coexist. Models also predicted high suitability for more than one species in Taberit *erg* (Mali; *A. longipes* and *A. dumerilii/senegalensis*), the Great Eastern Erg (Algeria; *A. longipes* and *A. scutellatus*) and the Afro-Arabian suture zone (Egypt; *A. aegyptius* and *A. scutellatus*).

3.4 | Population genetics and hybridization analysis

All samples from the PNBA sympatry zone were successfully genotyped for 14 microsatellite loci. Evidence of null alleles and

stuttering were revealed in, respectively, nine and six loci across the three clades recovered in the phylogenetic analyses, while no evidence of allelic dropout was found. No heterozygote excess was observed, while eight loci showed heterozygote deficiency across the clades. Two pairs of markers were found to significantly depart from linkage equilibrium. Considering this information, three markers were removed, resulting in a final filtered dataset of 11 markers (Table S2.13).

Delta K and L (K) methods recovered a best-supported number of clusters of K = 3 (Figure S1.11). No further coherent structuring was observed at higher K values. Structure analyses revealed three genetic clusters matching with the phylogenetic clades *A. aureus*, *A. dumerilii/senegalensis* and *A. longipes* (Figure 4). The pairwise F_{ST} values confirmed a high degree of genetic partitioning (Table S2.14). The three clusters were also clearly separated in the FCoA (Figure S1.12). No admixed individuals were apparent in the dataset and no differentiation between specimens morphologically identified as *A. dumerilii* or *A. senegalensis* (Table S2.1) was revealed by any analysis.

TABLE 1 GLMs of the effect of topography and soft-sand coverage on (a) mtDNA haplotype distinctiveness ($n = 421$; diversification model) and (b) lineage's range size ($n = 20$; connectivity model) of *Acanthodactylus scutellatus* group

(A) Haplotype distinctiveness	Coefficient	SE	t	p	(B) Lineage range size	Coefficient	SE	t	p
Intercept	7.1×10^{-4}	3.8×10^{-3}	0.2	0.85	Intercept	−682.7	1080.0	−0.6	0.54
Terrain roughness index	4.2×10^{-4}	8.2×10^{-5}	5.1	<0.01	Terrain roughness index	−1.2	72.9	0.0	0.99
Erg coverage	-4.6×10^{-4}	2.0×10^{-3}	−0.2	0.82	Erg coverage	61.23	19.4	3.2	<0.01
Nearest-neighbour distance	4.5×10^{-3}	8.0×10^{-4}	5.6	<0.01	N of lineage' samples	3.8	4.8	0.8	0.44
A. aureus	4.6×10^{-3}	4.4×10^{-3}	1.0	0.30	*A. aureus*	883.6	1093.2	0.8	0.44
A. dumerilii/senegalensis	2.6×10^{-3}	3.9×10^{-3}	0.7	0.51	*A. dumerilii/ senegalensis*	875.5	1159.3	0.8	0.47
A. longipes	3.8×10^{-3}	4.1×10^{-3}	0.9	0.35	*A. longipes*	286.6	1099.7	0.3	0.80
A. scutellatus	2.0×10^{-2}	4.2×10^{-3}	4.8	<0.01	*A. scutellatus*	712.3	975.6	0.7	0.48
A. taghitensis	2.3×10^{-3}	7.6×10^{-3}	−0.3	0.76	*A. taghitensis*	841.8	1165.6	0.7	0.49

Note: Significant results ($p < 0.01$) are highlighted in bold.
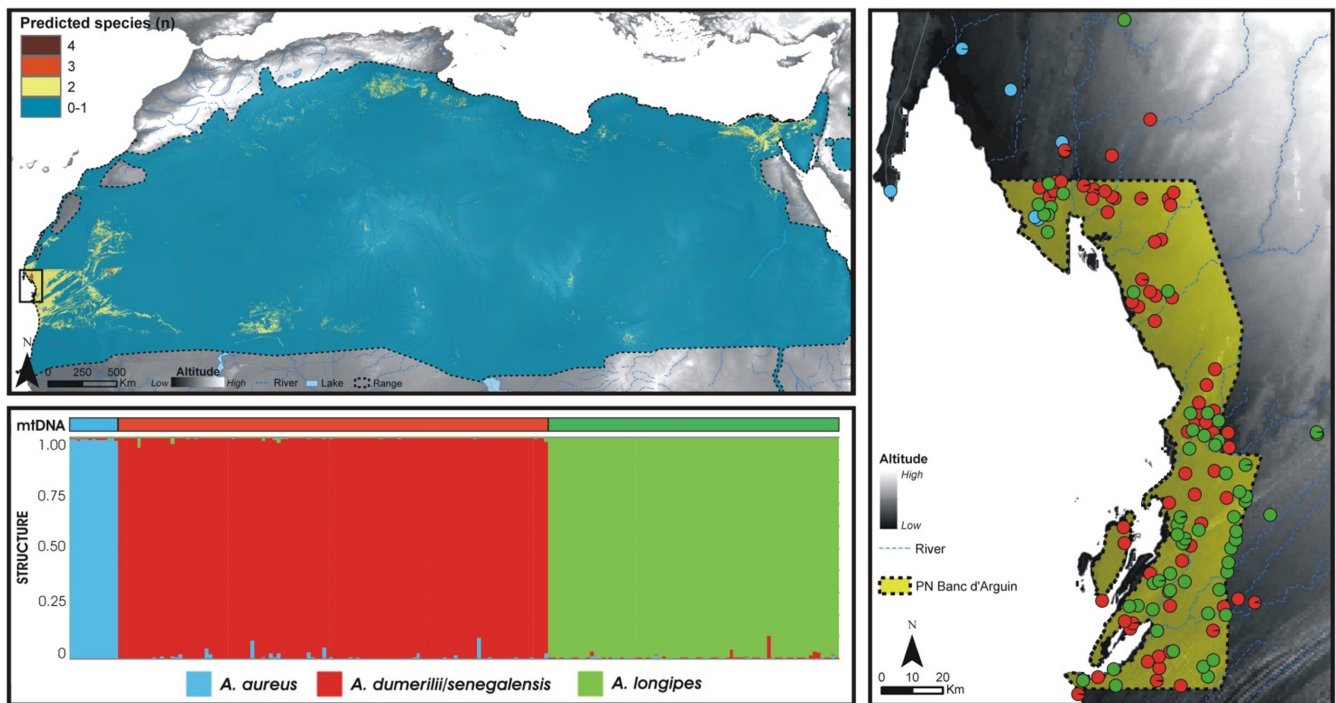

FIGURE 4 Top: Sympatry zones within *Acanthodactylus scutellatus* group, derived from the overlap of binary projections of species' ecological niche models. Right: Population structure of the group in the sympatry zone Parc National du Banc d'Arguin for the optimal number of clusters (K = 3), based on 11 microsatellite loci using Structure. Map projections: WGS84. Bottom: Structure bar plots of the individual's assignment to each cluster, in relation to mtDNA assignments. Vertical bars represent single individuals.

4 | DISCUSSION

4.1 | Overlooked species diversity in the hyper-arid Sahara Desert

The amount of diversity uncovered in this work clearly refutes the idea of biological homogeneity in hyper-arid desert habitats, which was assumed across the Sahara for the Scutellatus group due to the lack of morphological differentiation unveiled in early studies (Arnold, 1983; Salvador, 1982). Indeed, our phylogeographic assessment revealed high levels of unrecognized evolutionary diversity: several lineages that are embedded within broader-named species based on current taxonomy diverged before the Pleistocene (Figure 2) and are thus candidates for species-level status (see below). Among these candidate

lineages, only *A. aegyptius* has been formally recognized, based on its distinctive morphology and lack of intergradation in its narrow contact zone with *A. longipes* (Baha el Din, 2007).

The *A. longipes* clade includes two lineages ('Tunisia' and 'Grand Western Erg') which are older and more genetically distinct than *A. aegyptius* (Figure 2; Figure S1.6b; Table S2.9), suggesting that they constitute valid species. Species-level status is supported by private and well-differentiated nuclear haplotypes in relation to those of other closely distributed lineages (Figure S1.7a). Similarly, the *A. scutellatus* clade includes four lineages ('Nile Delta', 'Atlas High Plateau', 'Tassili-N'Ajjer' and 'Tunisia Coast') that point to cryptic species. These lineages show no signs of nuclear admixture in spite of their adjacent or even locally overlapping distributions (e.g. 'Tunisia Coast' lineage; Figures S1.7b and S1.7c). In some cases, their haplotypes appear clearly separated from the rest in the nuclear network ('Nile Delta' and 'Tunisia Coast'), whereas their mtDNA distances reach ~5% ('Nile Delta' and 'Tassili-N'Ajjer'; Table S2.9). Among them, the most evident candidate species is the Miocene-splitting lineage 'Nile Delta' (Figure 2), whose nuclear haplotypes are clearly differentiated from those of the other three co-distributed lineages in the Afro-Arabian suture zone (Figure S1.7c). The high diversity within *A. longipes* and *A. scutellatus* mirrors the patterns recovered in other Sahara-Sahel range-wide species (e.g., *Ptyodactylus togoensis* [Metallinou et al., 2015], *Tropiocolotes tripolitanus* [Machado et al., 2020]), although the number of candidate species is much higher in the case of these sand specialists.

The *A. dumerilii/senegalensis* and *A. taghitensis* clades present deep splits with similar timing in the Early Pliocene (Figure 2). The resulting lineages occur in allopatry without evidence of recent contact, given their well-differentiated nuclear haplotypes (Figure S1.6) and high mtDNA distances (Table S2.9). Further studies should assess the extent of reproductive isolation between these allopatric lineages, to determine whether they constitute real speciation events and which underlying processes were involved (e.g., neutral evolution in isolation by distance [Irwin, 2002]).

4.2 | Diversification hotspots and drivers of xeric diversity

The northern edge of the Sahara concentrates the highest levels of diversity, harbouring a patchwork of small-ranged endemic lineages consistent across local species (Figure 3; Figures S1.7d–S1.7f). Considering the seemingly parapatric distribution of these lineages, their mtDNA distinctiveness (Figure 3) and crown ages concordant with Saharan dry/humid cycles occurring since the Late Miocene (Figure 2; Zhang et al., 2014), the recovered phylogeographic patterns may be the result of historical episodes of population isolation (Brito et al., 2014). In the north-western side, rivers flowing from the southern foothills of the Saharan Atlas during humid phases could create barriers to gene flow by fragmenting sandy habitats across Algerian *ergs* (Scerri et al., 2014), like previously suggested for other sand-adapted taxa (e.g., *Chalcides ocellatus* [Beddek et al., 2018]). The increased humidity that allows intermittent north–south dispersal for more mesic species (e.g., *Psammophis schokari* [Gonçalves, Martínez-Freiría, et al., 2018]) may have created barriers to dryland-adapted taxa. An alternative

scenario to barriers is range shifts following climatic fluctuations, triggering genetic differentiation in allopatry (e.g., *Daboia* spp. [Martínez-Freiría et al., 2017]). In the Afro-Arabian suture zone, the observed divergence may also result from a dynamic tectonic history, which has been linked to speciation events and continental translocations of Afro-Arabian fauna (Tejero-Cicuéndez et al., 2022).

In other taxa, lineages endemic to Sahara highlands have highlighted the role of topography and local climate stability in generating diversity (e.g., *Acanthodactylus boskianus* [Liz et al., 2021]). While mountain habitats are far from the ecological optima of xeric species, their refugia may be located in mountain outskirts as a way to avoid the extreme climatic cores of the hyper-arid lowlands. Our models predict the suitability of mountain outskirts and mid-altitude environments for *A. scutellatus* (Figure S1.8), which seems to be able to disperse across mountain barriers (lineage 'Atlas High Plateau'; Figures S1.7b), as well as *A. longipes* (lineage 'Great Western Erg'; Figure S1.7a). These two species and *A. dumerilii/senegalensis* present high genetic variability around mountains areas, as shown by mtDNA haplotype distinctiveness south of the High Atlas, around Saharan Atlas, Fezzan and Adrar (Figure 3), by diverse nuclear haplotypes around the High and Saharan Atlas (Figures S1.7a and S1.7b), and by a seemingly endemic lineage to Tassili-N'Ajjer (Figure 2). We found a positive, significant relationship between terrain roughness and haplotype distinctiveness, supporting the mountain-outskirt xeric refugia hypothesis (Figure 3; Table 1). Nevertheless, conclusions are limited by the biased sampling across the study area, while the observed phylogeographic patterns can also result from long-term population persistence and divergence in the edge of nearby *erg* habitats, triggered by a favourable combination of environmental drivers (e.g., milder climate, habitat fragmentation). Fine-scale studies assessing diversification and palaeo-range patterns across mountain-*erg* geographic gradients are needed to further understand xeric refugia.

4.3 | Population connectivity and expansions across sand corridors

A pattern of large longitudinal genetic connectivity was recovered across southern latitudes (Figure 3), where lineages of *A. dumerilii/senegalensis*, *A. longipes* and *A. scutellatus* exhibit east–west distributions from Central Sahara-Sahel regions to the Red Sea and Atlantic coasts, including one lineage ('Pansaharan') ranging over an almost complete trans-Saharan axis. Connectivity was significantly favoured by soft-sand substrate (Figure 3; Table 1), which is recovered as a main driver of habitat suitability for range-wide species (e.g., *A. longipes*; Table S2.12). Our findings corroborate the hypothesis of recent longitudinal sand corridors across southern desert regions, previously suggested by lineage distributions from the Central Sahara to the Atlantic coast in other sand-adapted species (e.g., *Mesalina pasteuri*; *M. rubropunctata* [Pizzigalli et al., 2021]; *Stenodactylus petrii*, *S. sthenodactylus* [Metallinou et al., 2012]) and by similar trans-Saharan distributions of xeric species (e.g. *Uromastyx dispar* [Tamar

et al., 2017]). These corridors would explain the rapid desert colonization of sand specialists (e.g., *Scincus* spp. [Šmíd et al., 2020]), where intermittent dispersals were potentially followed by climate-induced allopatric diversification in northern latitudes (Brito et al., 2014).

The lack of accurate spatially explicit geological and land cover data for the past hinders inferences on the historical fluctuation of sand corridors and the direction of dispersals. Yet, areas of relatively high mtDNA haplotype distinctiveness within a given lineage distribution would imply long-term local population persistence (Carnaval et al., 2009), while distant areas sharing closely related haplotypes would suggest recent expansion. The *A. dumerilii/senegalensis* lineage 'W Sahara-Sahel south' is a good candidate to explore these patterns, since it is well sampled and associated with presumed xeric corridors (Figure 2). Potential dispersal origins are inferred around the Assaba and Afollé mountains, the Aouker *erg* and palaeolakes (Mauritania) and Taberit *erg* (Mali), from where lineage populations expanded north and westwards towards the Atlantic Sahara, and eastwards until the Lake Chad (Figure 3). A similar scenario of dispersal from inland areas may apply to lineage 'Pansaharan' (*A. scutellatus*), which likely expanded from Ténéré *erg* (Niger) westwards until Mauritania. Likewise, populations of lineage 'E Sahara-Sahel' (*A. longipes*) are distinctive around Bilma *erg* (Niger), which contrasts with potential areas of recent expansion in Chad and Egypt.

4.4 | Hybridization assessment and systematic clarifications

Population genetic analyses conducted within the main sympatry zone of the Scutellatus group (PNBA) indicated no gene flow among the three local species (Figure 4), despite suspicions of interspecific hybridization in the area (Crochet et al., 2003). The range of estimated F_{ST} values (Table S2.14) and separation of the FCoA clusters (Figure S1.12) is concordant with the deep phylogenetic split observed between these groups. The simplest explanation for the absence of gene flow is a speciation process largely predating the development of the sympatry zone (Figure 2). The area underwent historical climatic and land cover fluctuations, including the intermittent activation of the estuary of the giant Palaeoriver Tamanrasset during humid Sahara phases (Skonieczny et al., 2015), and offers a diverse ecotone (e.g., humidity, sand substrate) for the co-occurrence of closely related species. Ecological segregation between species is supported by different species ecological preferences (Table S2.12).

The genetic structure observed across PNBA supports the synonymy of *A. senegalensis* and *A. dumerilii* suggested by Tamar et al. (2016). Morphological assessments differentiate two local morphotypes, each assigned to an independent species (Table S2.1), based on differences in scalation and colour pattern (i.e., number of longitudinal rows of dorsal and ventral scales, number of femoral pores and presence of vertebral line; Crochet et al., 2003). Our genetic analyses lumped both morphotypes, as well as putative hybrids, into one single nuclear cluster (Figure 4; Figure S1.12). In addition, samples from the entire range of *A. senegalensis* and the southern range of *A. dumerilii* are integrated within a single mtDNA lineage (Figure 2). Therefore, the two morphotypes co-occurring in coastal Mauritania (Crochet et al., 2003) seem to result from a large morphological plasticity or variability within this single species.

Our results do not support the distribution of *A. dumerilii* as it is currently recognized on its northern range eastwards from Taghit (Algeria) to coastal Libya (Roll et al., 2017). The north-easternmost points where we identified *A. dumerilii* are around Taghit and Béchar (Algeria; Figure 2). Further east, all samples show either *A. scutellatus* or *A. longipes* nuclear haplotypes (Figures S1.7a and S1.7b). Westwards from Taghit, the links between two local lineages of *A. dumerilii/senegalensis* and *A. scutellatus* in the nuclear network (Figure S1.5) raise uncertainties on the identification of these two lineages. Nevertheless, the occurrence of *A. dumerilii* in this region is well supported, according to the mtDNA and nuclear placement of lineage 'Merzouga'. An updated range for *A. dumerilii/senegalensis* is provided in Appendix S4.

CONFLICT OF INTEREST

None.

DATA AVAILABILITY STATEMENT

GenBank accession numbers and sampling localities are indicated in Table S2.1.

ORCID

André Vicente Liz https://orcid.org/0000-0001-6131-5194
Dennis Rödder https://orcid.org/0000-0002-6108-1639
Duarte Vasconcelos Gonçalves https://orcid.org/0000-0003-4299-0375
Guillermo Velo-Antón https://orcid.org/0000-0002-9483-5695
Pedro Tarroso https://orcid.org/0000-0002-2694-1170
Pierre-André Crochet https://orcid.org/0000-0002-0422-3960
Silvia B. Carvalho https://orcid.org/0000-0003-4368-4708
José Carlos Brito https://orcid.org/0000-0001-5444-8132

REFERENCES

Aiello-Lammens, M. E., Boria, R. A., Radosavljevic, A., Vilela, B., & Anderson, R. P. (2015). SpThin: An R package for spatial thinning of species occurrence records for use in ecological niche models. *Ecography*, *38*, 541–545. https://doi.org/10.1111/ecog.01132

Akaike, H. (1998). Information theory and an extension of the maximum likelihood principle. In E. Parzen, K. Tanabe, & G. Kitagawa (Eds.), *Selected Papers of Hirotugu Akaike. Springer series in Statistics*. Springer. https://doi.org/10.1007/978-1-4612-1694-0_15

Arnold, E. N. (1983). Osteology, genitalia and the relationships of *Acanthodactylus* (Reptilia: Lacertidae). *Bulletin of the British Museum (Natural History) Zoology*, *44*, 291–339.

Baha El Din, S. M. (2007). A new lizard of the *Acanthodactylus scutellatus* group (Squamata: Lacertidae) from Egypt. *Zoology in the Middle East*, *40*, 21–32. https://doi.org/10.1080/09397140.2007.10638200

Barkley, A. E., Pourmand, A., Longman, J., Sharifi, A., Prospero, J. M., Panechou, K., Bakker, N., Drake, N., Guinoiseau, D., & Gaston, C. J. (2022). Interannual variability in the source location of north African dust transported to the Amazon. *Geophysical Research Letters*, e2021GL097344. https://doi.org/10.1029/2021GL097344

Beddek, M., Zenboudji-Beddek, S., Geniez, P., Fathalla, R., Sourouille, P., Arnal, V., Dellaoui, B., Koudache, F., Telailia, S., Peyre, O., & Crochet, P. A. (2018). Comparative phylogeography of amphibians and reptiles in Algeria suggests common causes for the east-west phylogeographic breaks in the Maghreb. *PLoS One*, *13*, e0201218. https://doi.org/10.1371/journal.pone.0201218

Bicheron, P., Defourny, P., Brockmann, C., Schouten, L., Vancutsem, C., Huc, M., Sophie, B., Marc, L., Frederic, A., Martin, H., Frank, R., & Olivier, A. (2009). *GLOBCOVER products description and validation report*. Technical Report. Medias France.

Boria, R. A., Olson, L. E., Goodman, S. M., & Anderson, R. P. (2014). Spatial filtering to reduce sampling bias can improve the performance of ecological niche models. *Ecological Modelling*, *275*, 73–77. https://doi.org/10.1016/j.ecolmodel.2013.12.012

Brito, J. C., Durant, S. M., Pettorelli, N., Newby, J., Canney, S., Algadafi, W., Rabeil, T., Crochet, P.-A., Pleguezuelos, J. M., Wacher, T., de Smet, K., Gonçalves, D. V., da Silva, M. J. F., Martínez-Freiría, F., Abáigar, T., Campos, J. C., Comizzoli, P., Fahd, S., Fellous, A., … Carvalho, S. B. (2018). Armed conflicts and wildlife decline: Challenges and recommendations for effective conservation policy in the Sahara-Sahel. *Conservation Letters*, *11*, e12446. https://doi.org/10.1111/conl.12446

Brito, J. C., Godinho, R., Martínez-Freiría, F., Pleguezuelos, J. M., Rebelo, H., Santos, X., Vale, C. G., Velo-Antón, G., Boratyński, Z., Carvalho, S. B., Ferreira, S., Gonçalves, D. V., Silva, T. L., Tarroso, P., Campos, J. C., Leite, J. V., Nogueira, J., Alvares, F., Sillero, N., … Carranza, S. (2014). Unravelling biodiversity, evolution and threats to conservation in the Sahara-Sahel. *Biological Reviews*, *89*, 215–231. https://doi.org/10.1111/brv.12049

Brito, J. C., & Pleguezuelos, J. M. (2020). Desert biodiversity—world's hot spots/globally outstanding biodiverse deserts. *Encyclopedia of the World's Biomes*, *2*, 10–22. https://doi.org/10.1016/B978-0-12-409548-9.11794-4

Brito, J. C., Tarroso, P., Vale, C. G., Martínez-Freiría, F., Boratyński, Z., Campos, J. C., Ferreira, S., Godinho, R., Gonçalves, D. V., Leite, J. V., Lima, V. O., Pereira, P., Santos, X., Ferreira da Silva, M. J., Silva, T. L., Velo-Antón, G., Veríssimo, J., Crochet, P.-A., Pleguezuelos, J. M., & Carvalho, S. B. (2016). Conservation biogeography of the Sahara-Sahel: Additional protected areas are needed to secure unique biodiversity. *Diversity and Distributions*, *22*, 371–384. https://doi.org/10.1111/ddi.12416

Carnaval, A. C., Hickerson, M. J., Haddad, C. F., Rodrigues, M. T., & Moritz, C. (2009). Stability predicts genetic diversity in the Brazilian Atlantic forest hotspot. *Science*, *323*, 785–789. https://doi.org/10.1126/science.1166955

Carranza, S., Arnold, E. N., Geniez, P., Roca, J., & Mateo, J. A. (2008). Radiation, multiple dispersal and parallelism in the skinks, *Chalcides* and *Sphenops* (Squamata: Scincidae), with comments on *Scincus* and *Scincopus* and the age of the Sahara Desert. *Molecular Phylogenetics and Evolution*, *46*, 1071–1094. https://doi.org/10.1016/j.ympev.2007.11.018

Clement, M. J., Snell, Q., Walker, P., Posada, D., & Crandall, K. A. (2002). TCS: Estimating gene genealogies. In *Proceedings of the 16th international parallel and distributed processing symposium 2* (p. 184). Washington, DC: Institute of Electrical and Electronics Engineers Computer Society.

Crochet, P. A., Geniez, P., & Ineich, I. (2003). A multivariate analysis of the fringe-toed lizards of the *Acanthodactylus scutellatus* group (Squamata: Lacertidae): Systematic and biogeographical implications. *Zoological Journal of the Linnean Society*, *137*, 117–155. https://doi.org/10.1046/j.1096-3642.2003.00044.x

Di Cola, V., Broennimann, O., Petitpierre, B., Breiner, F. T., d'Amen, M., Randin, C., Engler, R., Pottier, J., Pio, D., Dubuis, A., Pellissier, L., Mateo, R. G., Hordijk, W., Salamin, N., & Guisan, A. (2017). Ecospat: An R package to support spatial analyses and modeling of species niches and distributions. *Ecography*, *40*, 774–787. https://doi.org/10.1111/ecog.02671

Dinerstein, E., Olson, D., Joshi, A., Vynne, C., Burgess, N. D., Wikramanayake, E., Hahn, N., Palminteri, S., Hedao, P., Noss, R., Hansen, M., Locke, H., Ellis, E. C., Jones, B., Barber, C. V., Hayes, R., Kormos, C., Martin, V., Crist, E., … Saleem, M. (2017). An ecoregion-based approach to protecting half the terrestrial realm. *Bioscience*, *67*, 534–545. https://doi.org/10.1093/biosci/bix014

Drake, N. A., Blench, R. M., Armitage, S. J., Bristow, C. S., & White, K. H. (2011). Ancient watercourses and biogeography of the Sahara explain the peopling of the desert. *PNAS*, *108*, 458–462. https://doi.org/10.1073/pnas.1012231108

Drummond, A. J., Ho, S. Y. W., Phillips, M. J., & Rambaut, A. (2006). Relaxed phylogenetics and dating with confidence. *PLoS Biology*, *4*, e88. https://doi.org/10.1371/journal.pbio.0040088

Durant, S. M., Pettorelli, N., Bashir, S., Woodroffe, R., Wacher, T., De Ornellas, P., Ransom, C., Abáigar, T., Abdelgadir, M., El Alqamy, H., Beddiaf, M., Belbachir, F., Belbachir-Bazi, A., Berbash, A. A., Beudels-Jamar, R., Boitani, L., Breitenmoser, C., Cano, M., Chardonnet, P., … Baillie, J. E. (2012). Forgotten biodiversity in desert ecosystems. *Science*, *336*, 1379–1380. https://doi.org/10.1126/science.336.6087.1379

Durant, S. M., Wacher, T., Bashir, S., Woodroffe, R. D., De Ornellas, P., Ransom, C., Newby, J., Abáigar, T., Abdelgadir, M., El Alqamy, H., Baillie, J., Beddiaf, M., Belbachir, F., Belbachir-Bazi, A., Berbash, A. A., Bemadjim, N. E., Beudels-Jamar, R., Boitani, L., Breitenmoser, C., … Pettorelli, N. (2014). Fiddling in biodiversity hotspots while deserts burn? Collapse of the Sahara's megafauna. *Diversity and Distributions*, *20*, 114–122. https://doi.org/10.1111/ddi.12157

Elith, J., Kearney, M., & Phillips, S. (2010). The art of modelling range-shifting species. *Methods in Ecology and Evolution*, *1*, 330–342. https://doi.org/10.1111/j.2041-210X.2010.00036.x

ESRI. (2006). *ArcMap 10.5*. Environmental Systems Research Institute, Inc.

Fick, S. E., & Hijmans, R. J. (2017). WorldClim 2: New 1-km spatial resolution climate surfaces for global land areas. *International Journal of Climatology*, *37*, 4302–4315. https://doi.org/10.1002/joc.5086

Fielding, A. H., & Bell, J. F. (1997). A review of methods for the assessment of prediction errors in conservation presence/absence models. *Environmental Conservation*, *24*, 38–49. https://doi.org/10.1017/S0376892997000088

Gonçalves, D. V., Martínez-Freiría, F., Crochet, P. A., Geniez, P., Carranza, S., & Brito, J. C. (2018). The role of climatic cycles and trans-Saharan migration corridors in species diversification: Biogeography of *Psammophis schokari* group in North Africa. *Molecular Phylogenetics and Evolution*, *118*, 64–74. https://doi.org/10.1016/j.ympev.2017.09.009

Gonçalves, D. V., Pereira, P., Velo-Antón, G., Harris, D. J., Carranza, S., & Brito, J. C. (2018). Assessing the role of aridity-induced vicariance and ecological divergence in species diversification in north-West Africa using *agama* lizards. *Biological Journal of the Linnean Society*, *124*, 363–380. https://doi.org/10.1093/biolinnean/bly055

Harris, D. J., & Arnold, E. N. (2000). Elucidation of the relationships of spiny-footed lizards, *Acanthodactylus* spp.(Reptilia: Lacertidae) using mitochondrial DNA sequence, with comments on their biogeography and evolution. *Journal of Zoology*, *252*, 351–362. https://doi.org/10.1111/j.1469-7998.2000.tb00630.x

Huete, A. R., Liu, H., Batchily, K., & van Leeuwen, W. (1997). A comparison of vegetation indices over a global set of TM images for EOS-MODIS. *Remote Sensing of Environment*, *59*, 440–451. https://doi.org/10.1016/S0034-4257(96)00112-5

Hughes, A. C., Orr, M. C., Yang, Q., & Qiao, H. (2021). Effectively and accurately mapping global biodiversity patterns for different regions and taxa. *Global Ecology and Biogeography*, *30*, 1375–1388. https://doi.org/10.1111/geb.13304

Irwin, D. E. (2002). Phylogeographic breaks without geographic barriers to gene flow. *Evolution*, *56*, 2383–2394. https://doi.org/10.1111/j.0014-3820.2002.tb00164.x

Jensen, J. (2007). *Remote sensing of the environment: An earth resource perspective*. Pearson Education.

Kingman, J. F. C. (1982). The coalescent. *Stochastic Processes and their Applications*, *13*, 235–248. https://doi.org/10.1016/0304-4149(82)90011-4

Librado, P., & Rozas, J. (2009). DnaSP v5: A software for comprehensive analysis of DNA polymorphism data. *Bioinformatics*, *25*, 1451–1452. https://doi.org/10.1093/bioinformatics/btp187

Liz, A. V., Rödder, D., Gonçalves, D. V., Velo-Antón, G., Fonseca, M. M., Crochet, P. A., & Brito, J. C. (2021). The role of Sahara highlands in the diversification and desert colonisation of the Bosc's

fringe-toed lizard. *Journal of Biogeography*, *48*, 2891–2906. https://doi.org/10.1111/jbi.14250

Lopes, S. C., Velo-Antón, G., Pereira, P., Lopes, S., Godinho, R., Crochet, P. A., & Brito, J. C. (2015). Development and characterization of polymorphic microsatellite loci for spiny-footed lizards, *Acanthodactylus scutellatus* group (Reptilia, Lacertidae) from arid regions. *BMC Research Notes*, *8*, 1–10. https://doi.org/10.1186/s13104-015-1779-3

Machado, L., Salvi, D., Harris, D. J., Brito, J. C., Crochet, P. A., Geniez, P., Ahmadzadeh, F., & Carranza, S. (2020). Systematics, biogeography and evolution of the Saharo-Arabian naked-toed geckos genus *Tropiocolotes*. *Molecular Phylogenetics and Evolution*, *155*, 106969. https://doi.org/10.1016/j.ympev.2020.106969

Marmion, M., Parviainen, M., Luoto, M., Heikkinen, R. K., & Thuiller, W. (2009). Evaluation of consensus methods in predictive species distribution modelling. *Diversity and Distributions*, *15*, 59–69. https://doi.org/10.1111/j.1472-4642.2008.00491.x

Martínez-Freiría, F., Crochet, P. A., Fahd, S., Geniez, P., Brito, J. C., & Velo-Antón, G. (2017). Integrative phylogeographical and ecological analysis reveals multiple Pleistocene refugia for Mediterranean *daboia* vipers in north-West Africa. *Biological Journal of the Linnean Society*, *122*, 366–384. https://doi.org/10.1093/biolinnean/blx038

Matthiopoulos, J. (2011). *How to be a quantitative ecologist: The 'A to R' of green mathematics and statistics*. John Wiley & Sons.

Metallinou, M., Arnold, E. N., Crochet, P. A., Geniez, P., Brito, J. C., Lymberakis, P., El Din, S. B., Sindaco, R., Robinson, M., & Carranza, S. (2012). Conquering the Sahara and Arabian deserts: Systematics and biogeography of *Stenodactylus* geckos (Reptilia: Gekkonidae). *BMC Evolutionary Biology*, *12*, 1–17. https://doi.org/10.1186/1471-2148-12-258

Metallinou, M., Červenka, J., Crochet, P. A., Kratochvíl, L., Wilms, T., Geniez, P., Shobrak, M. Y., Brito, J. C., & Carranza, S. (2015). Species on the rocks: Systematics and biogeography of the rock-dwelling *Ptyodactylus* geckos (Squamata: Phyllodactylidae) in North Africa and Arabia. *Molecular Phylogenetics and Evolution*, *85*, 208–220. https://doi.org/10.1016/j.ympev.2015.02.010

Miller, M. A., Pfeiffer, W., & Schwartz, T. (2010). Creating the CIPRES Science Gateway for inference of large phylogenetic trees. In *2010 Gateway computing environments workshop, GCE 2010*. Manhattan, NY: Institute of Electrical and Electronics Engineers.

Paradis, E. (2010). Pegas: An R package for population genetics with an integrated–modular approach. *Bioinformatics*, *26*, 419–420. https://doi.org/10.1093/bioinformatics/btp696

Pepper, M., & Keogh, J. S. (2021). Life in the "dead heart" of Australia: The geohistory of the Australian deserts and its impact on genetic diversity of arid zone lizards. *Journal of Biogeography*, *48*, 716–746. https://doi.org/10.1111/jbi.14063

Pizzigalli, C., Crochet, P. A., Geniez, P., Martínez-Freiría, F., Velo-Antón, G., & Brito, J. C. (2021). Phylogeographic diversification of the *Mesalina olivieri* species complex (Squamata: Lacertidae) with the description of a new species and a new subspecies endemic from north West Africa. *Journal of Zoological Systematics and Evolutionary Research*, *59*, 2321–2349. https://doi.org/10.1111/jzs.12516

Pritchard, J. K., Stephens, M., Rosenberg, N. A., & Donnelly, P. (2000). Association mapping in structured populations. *American Journal of Human Genetics*, *67*, 170–181. https://doi.org/10.1086/302959

Psonis, N., Lymberakis, P., Poursanidis, D., & Poulakakis, N. (2016). Contribution to the study of *Acanthodactylus* (Sauria: Lacertidae) mtDNA diversity focusing on the *a. boskianus* species group. *Mitochondrion*, *30*, 78–94. https://doi.org/10.1016/j.mito.2016.07.001

Roll, U., Feldman, A., Novosolov, M., Allison, A., Bauer, A. M., Bernard, R., Böhm, M., Castro-Herrera, F., Chirio, L., Collen, B., Colli, G. R., Dabool, L., Das, I., Doan, T. M., Grismer, L. L., Hoogmoed, M.,

Itescu, Y., Kraus, F., LeBreton, M., … Meiri, S. (2017). The global distribution of tetrapods reveals a need for targeted reptile conservation. *Nature Ecology and Evolution*, 1, 1677–1682. https://doi.org/10.1038/s41559-017-0332-2

Rousset, F. (2008). GENEPOP'007: A complete re-implementation of the genepop software for windows and Linux. *Molecular Ecology Resources*, 8, 103–106. https://doi.org/10.1111/j.1471-8286.2007.01931.x

Salvador, A. (1982). A revision of the lizards of the genus *Acanthodactylus* (Sauria: Lacertidae). *Bonner Zoologische Monographien*, 16, 1–167.

Santos, A. M., Cabezas, M. P., Tavares, A. I., Xavier, R., & Branco, M. (2015). TcsBU: A tool to extend TCS network layout and visualization. *Bioinformatics*, 32, 627–628. https://doi.org/10.1093/bioinformatics/btv636

Scerri, E. M., Drake, N. A., Jennings, R., & Groucutt, H. S. (2014). Earliest evidence for the structure of *Homo sapiens* populations in Africa. *Quaternary Science Reviews*, 101, 207–216. https://doi.org/10.1016/j.quascirev.2014.07.019

Silvestro, D., & Michalak, I. (2012). raxmlGUI: A graphical front-end for RAxML. *Organisms, Diversity and Evolution*, 12, 335–337. https://doi.org/10.1007/s13127-011-0056-0

Sindaco, R., & Jeremčenko, V. K. (2008). *The reptiles of the Western palearctic: Annotated checklist and distributional atlas of the turtles, crocodiles, amphisbaenians and lizards of Europe, North Africa*. Middle East and Central Asia.

Skonieczny, C., Paillou, P., Bory, A., Bayon, G., Biscara, L., Crosta, X., Eynaud, F., Malaizé, B., Revel, M., Aleman, N., Barusseau, J.-P., Vernet, R., Lopez, S., & Grousset, F. (2015). African humid periods triggered the reactivation of a large river system in Western Sahara. *Nature Communications*, 6, 1–6. https://doi.org/10.1038/ncomms9751

Šmíd, J., Sindaco, R., Shobrak, M., Busais, S., Tamar, K., Aghova, T., Simó-Riudalbas, M., Tarroso, P., Geniez, P., Crochet, P.-A., Els, J., Burriel-Carranza, B., Tejero-Cicuéndez, H., & Carranza, S. (2021). Diversity patterns and evolutionary history of Arabian squamates. *Journal of Biogeography*, 48, 1183–1199. https://doi.org/10.1111/jbi.14070

Šmíd, J., Uvizl, M., Shobrak, M., Salim, A. L. A., AlGethami, R. H. M., Algethami, A. R., ASK, A., Alsubaie, S. D., Busais, S., & Carranza, S. (2020). Swimming through the sands of the Sahara and Arabian deserts: Phylogeny of sandfish skinks (Scincidae, *Scincus*) reveals a recent and rapid diversification. *Molecular Phylogenetics and Evolution*, 155, 107012. https://doi.org/10.1016/j.ympev.2020.107012

Soultan, A., Wikelski, M., & Safi, K. (2019). Risk of biodiversity collapse under climate change in the afro-Arabian region. *Scientific Reports*, 9, 1–12. https://doi.org/10.1038/s41598-018-37851-6

Steele, T. E. (2007). In Late Pleistocene of Africa. In S. A. Elias & C. J. Mock (Eds.), *Encyclopedia of quaternary science* (pp. 3139–3150). Elsevier. https://doi.org/10.1016/b978-0-444-53643-3.00247-8

Suchard, M. A., Lemey, P., Baele, G., Ayres, D. L., Drummond, A. J., & Rambaut, A. (2018). Bayesian phylogenetic and phylodynamic data integration using BEAST 1.10. *Virus Evolution*, 4, vey016. https://doi.org/10.1093/ve/vey016

Tamar, K., Carranza, S., Sindaco, R., Moravec, J., & Meiri, S. (2014). Systematics and phylogeography of *Acanthodactylus schreiberi* and its relationships with *Acanthodactylus boskianus* (Reptilia: Squamata: Lacertidae). *Zoological Journal of the Linnean Society*, 172, 720–739. https://doi.org/10.1111/zoj.12170

Tamar, K., Carranza, S., Sindaco, R., Moravec, J., Trape, J. F., & Meiri, S. (2016). Out of Africa: Phylogeny and biogeography of the widespread genus *Acanthodactylus* (Reptilia: Lacertidae). *Molecular Phylogenetics and Evolution*, 103, 6–18. https://doi.org/10.1016/j.ympev.2016.07.003

Tamar, K., Metallinou, M., Wilms, T., Schmitz, A., Crochet, P. A., Geniez, P., & Carranza, S. (2017). Evolutionary history of spiny-tailed lizards (Agamidae: *Uromastyx*) from the Saharo-Arabian region. *Zoologica Scripta*, 47, 159–173. https://doi.org/10.1111/zsc.12266

Tamura, K., Stecher, G., Peterson, D., Filipski, A., & Kumar, S. (2013). MEGA6: Molecular evolutionary genetics analysis version 6.0. *Molecular Biology and Evolution*, 30, 2725–2729. https://doi.org/10.1093/molbev/mst197

Tarroso, P., Carvalho, S. B., & Velo-Antón, G. (2019). Phylin 2.0: Extending the phylogeographic interpolation method to include uncertainty and user-defined distance metrics. *Molecular Ecology Resources*, 19, 1081–1094. https://doi.org/10.1111/1755-0988.13010

Tejero-Cicuéndez, H., Patton, A., Caetano, D., Šmíd, J., Harmon, L., & Carranza, S. (2022). Reconstructing squamate biogeography in afro-Arabia reveals the influence of a complex and dynamic geologic past. *Systematic Biology*, 71, 261–272. https://doi.org/10.1093/sysbio/syab025

Thuiller, W., Georges, D., Engler, R., Breiner, F., 2021. Package "biomod 2" version 2.1.15. Available at: http://cran.r-project.org/web/packages/biomod2/biomod2.pdf

Thuiller, W., Guéguen, M., Renaud, J., Karger, D. N., & Zimmermann, N. E. (2019). Uncertainty in ensembles of global biodiversity scenarios. *Nature Communications*, 10, 1–9. https://doi.org/10.1038/s41467-019-09519-w

Title, P. O., & Bemmels, J. B. (2018). ENVIREM: An expanded set of bioclimatic and topographic variables increases flexibility and improves performance of ecological niche modelling. *Ecography*, 41, 291–307. https://doi.org/10.1111/ecog.02880

Tucker, C. J. (1979). Red and photographic infrared linear combinations for monitoring vegetation. *Remote Sensing of Environment*, 8, 127–150.

Van Oosterhout, C., Hutchinson, W. F., Wills, D. P., & Shipley, P. (2004). MICRO-CHECKER: Software for identifying and correcting genotyping errors in microsatellite data. *Molecular Ecology Notes*, 4, 535–538. https://doi.org/10.1111/j.1471-8286.2004.00684.x

Velo-Antón, G., Henrique, M., Liz, A. V., Martínez-Freiría, F., Pleguezuelos, J. M., Geniez, P., Crochet, P.-A., & Brito, J. C. (2022). DNA barcode reference library for the West Sahara-Sahel reptiles. *Scientific Data*, 9, 459. https://doi.org/10.1038/s41597-022-01582-1

Velo-Antón, G., Martínez-Freiría, F., Pereira, P., Crochet, P. A., & Brito, J. C. (2018). Living on the edge: Ecological and genetic connectivity of the spiny-footed lizard, *Acanthodactylus aureus*, confirms the Atlantic Sahara desert as a biogeographic corridor and Centre of lineage diversification. *Journal of Biogeography*, 45, 1031–1042. https://doi.org/10.1111/jbi.13176

Ward, D. (2016). *The biology of deserts*. Oxford University Press.

Weiss, D. J., Nelson, A., Gibson, H. S., Temperley, W., Peedell, S., Lieber, A., Hancher, M., Poyart, E., Belchior, S., Fullman, N., Mappin, B., Dalrymple, U., Rozier, J., TCD, L., Howes, R. E., Tusting, L. S., Kang, S. Y., Cameron, E., Bisanzio, D., … Gething, P. W. (2018). A global map of travel time to cities to assess inequalities in accessibility in 2015. *Nature*, 553, 333–336. https://doi.org/10.1038/nature25181

Yang, W., Feiner, N., Pinho, C., While, G. M., Kaliontzopoulou, A., Harris, D. J., Salvi, D., & Uller, T. (2021). Extensive introgression and mosaic genomes of Mediterranean endemic lizards. *Nature Communications*, 12, 1–8. https://doi.org/10.1038/s41467-021-22949-9

Zhang, Z., Ramstein, G., Schuster, M., Li, C., Contoux, C., & Yan, Q. (2014). Aridification of the Sahara desert caused by Tethys Sea shrinkage during the late Miocene. *Nature*, 513, 401–404. https://doi.org/10.1038/nature13705

BIOSKETCH

André Vicente Liz is a Ph.D. candidate at CIBIO-InBIO (University of Porto, Portugal) and Zoological Research Museum Alexander Koenig (Bonn, Germany), and is interested in biogeographic approaches to conservation. His Ph.D. project aims to understand the role of climate-induced dispersal/vicariance as main biodiversity diversification drivers in the Sahara-Sahel desert, based on comparative phylogeography. All authors are interested in the assessment of biodiversity patterns and processes in deserts and arid regions.

Author contributions: AVL, DR, DVG and JCB conceived the ideas; AVL, DVG, GVA, JCB, PAC and PG collected the data; AVL, DR, DVG, GVA, PAC, PT and SBC analysed the data; AVL led the writing with inputs from all authors.

SUPPORTING INFORMATION

Additional supporting information can be found online in the Supporting Information section at the end of this article.